Magnetic Materials

DOI: 10.1002/anie.200703010

A Millimeter-Wave Absorber Based on Gallium-Substituted ε-Iron Oxide Nanomagnets**

Shin-ichi Ohkoshi, Shiro Kuroki, Shunsuke Sakurai, Kazuyuki Matsumoto, Kimitaka Sato, and Shinya Sasaki*

Electromagnetic (EM) waves in the millimeter wave range (30–300 GHz) are beginning to be used in electronic devices for high-speed wireless communication such as in local-area networks and radars for the distance between cars.[1] Particularly, millimeter waves at frequencies of 35, 94, and 140 GHz have high transparency in the air (the so-called window of the air) and are useful for wireless communication. The development of complementary metal oxide semiconductor devices has also accelerated the use of EM waves in these bands.[2] However, currently materials that effectively restrain electromagnetic interference (EMI) in the region of millimeter waves almost do not exist.[3] Thus, finding a suitable material has received much attention. Insulating magnetic materials absorb EM waves owing to ferromagnetic resonance. Particularly, a magnetic material with a large coercive field (H_c) is expected to show a high-frequency resonance. In recent years, a single phase of ε-Fe_2O_3 nanomagnet has been isolated. This nanomagnet has an extremely large H_c value of 20 kOe at room temperature.[4–7] Herein, we report a new EM absorber composed of ε-$Ga_xFe_{2-x}O_3$ ($0.10 \le x \le 0.67$) nanomagnets, which shows a ferromagnetic resonance in the region of 35–147 GHz. In addition, the possibility that the ferromagnetic resonance can achieve a frequency of about 190 GHz at $x \to 0$ is also suggested.

A new series of ε-$Ga_xFe_{2-x}O_3$ ($0.10 \le x \le 0.67$) nanoparticles was synthesized by the combination of reverse-micelle and sol–gel techniques or only the sol–gel method (see the Experimental Section). In the TEM image of the sample for $x = 0.61$, sphere-type particles with a particle size of 39 ± 16 nm are observed as shown in Figure 1 a. In addition, the TEM images of other compositional materials are composed of similar types of nanoparticles (Figure S1 in the Supporting Information). Rietveld analyses of XRD patterns indicate that the material of this series has an orthorhombic

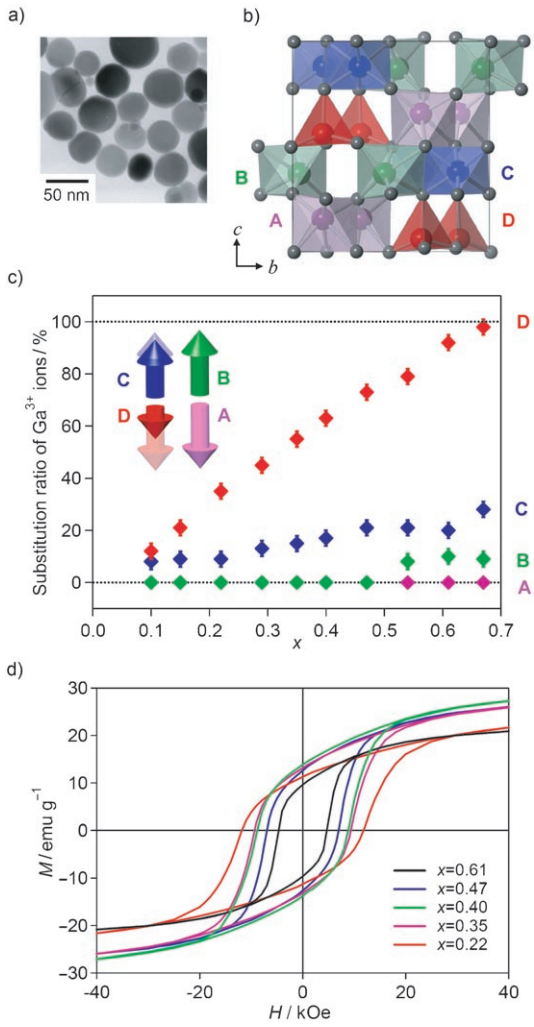

Figure 1. Crystal structures and magnetic properties of ε-$Ga_xFe_{2-x}O_3$. a) TEM image for $x = 0.61$. b) Crystal structure of $x = 0.61$ (space group: $Pna2_1$) projected from the [100] direction. Purple, green, and blue octahedra represent {FeO_6} units of the A, B, and C sites, respectively, while the red tetrahedra represent {FeO_4} units of the D site. c) The x dependence on the degree of Ga^{3+} substitution at the A (purple), B (green), C (blue), and D sites (red); the inset is a schematic diagram of the magnetic ordering of sublattice magnetization on A–D sites. d) Magnetization vs. external magnetic field plots for $x = 0.22$, 0.35, 0.40, 0.47, and 0.61 at 300 K.

[*] Prof. S. Ohkoshi, S. Kuroki, S. Sakurai
Department of Chemistry
School of Science
The University of Tokyo
7-3-1 Hongo, Bunkyo-ku, Tokyo 113-0033 (Japan)
Fax: (+81) 3-3812-1896
E-mail: ohkoshi@chem.s.u-tokyo.ac.jp
K. Matsumoto, K. Sato, S. Sasaki
Dowa Electronics Materials. Co., Ltd.
1-3-1 Kaigandori, Okayama 702–8506 (Japan)

[**] The authors thank Prof. K. Hashimoto for helpful discussions and T. Matsuda for preparing the color illustration. The present research herein is supported in part by a Grant-in-Aid for Scientific Research from the Ministry of Education, Culture, Sports, Science and Technology of Japan, JSPS, and RFBR under the Japan–Russia Research Cooperative Program, as well as Yamada Science Foundation, the Asahi Glass Foundation, the Kurata Memorial Hitachi Science and Technology Foundation, and the Murata Science Foundation.

Supporting information for this article is available on the WWW under http://www.angewandte.org or from the author.

crystal structure in the $Pna2_1$ space group (Figure S2 in the Supporting Information). This crystal structure has four non-equivalent Fe sites (A–D), that is, the coordination geometries of the A–C sites are octahedral $\{FeO_6\}$ units and those of the D sites are tetrahedral $\{FeO_4\}$ units (Figure 1b). For example, in the case of $x = 0.61$, 92% of the D sites and 20% of the C sites are substituted by Ga^{3+} ions, but the A and B sites are not substituted because Ga^{3+} (0.620 Å), which has a smaller ionic radius than Fe^{3+} (0.645 Å),[8] is preferentially located in the tetrahedral sites. The lattice constants for these samples are systematically compressed as the x value increases (Table S1 in the Supporting Information). Figure 1c exhibits plots of the degree of Ga^{3+} substitution as a function of x.

The magnetic properties of this series are listed in Table S2 in the Supporting Information. The field-cooled magnetization curves in an external magnetic field of 10 Oe show that the T_c value monotonously decreases from 492 K ($x = 0.10$) to 324 K ($x = 0.67$) as x increases (Figure S3 in the Supporting Information). Figure 1d shows the magnetization versus external magnetic field plots for $x = 0.22$, 0.35, 0.40, 0.47, and 0.61 at 300 K. The plots for other compositional materials are shown in Figure S4 in the Supporting Information. The H_c value decreases from 15.9 kOe ($x = 0.10$) to 2.1 kOe ($x = 0.67$). The saturation magnetization (M_s) value at 90 kOe increases from 14.9 emu g^{-1} ($x = 0.10$) to 30.1 ($x = 0.40$) and then decreases to 17.0 ($x = 0.67$). The magnetization versus external magnetic field plots at 2 K (Figure S4 in the Supporting Information) show the magnetic ordering of the sublattice magnetization of the A–D sites. As shown in the insert of Figure 1c, ε-$Ga_xFe_{2-x}O_3$ exhibits ferrimagnetic ordering such that the sublattice magnetizations at the A and D sites (M_A and M_D) are ordered antiparallel relative to those at the B and C sites (M_B and M_C). By using the distribution of Ga^{3+} substitution from the Rietveld analyses, the expected M_s value at 0 K is expressed as $M_s = 0.5(-aM_A + bM_B + cM_C - dM_D)$ where a–d are the respective Fe^{3+} ion contents at the A–D sites. The expected M_s values agree with the observed M_s values at 2 K as shown in Figure S5 in the Supporting Information.

The EM absorption properties in the range of 50–110 GHz were measured at room temperature by the free-space method (Figure 2a; see the Experimental Section). The samples between $x = 0.61$ and 0.29 show strong absorption in this range (Figure 2b). The sample for $x = 0.61$ shows a strong absorption at 54 GHz. As x decreases, the frequency of the absorption peak shifts to a higher one, that is, 64 GHz ($x = 0.54$), 73 GHz ($x = 0.47$), 84 GHz ($x = 0.40$), 88 GHz ($x = 0.35$), and 97 GHz ($x = 0.29$). In the samples for $x = 0.67$, 0.22, 0.15, and 0.10, the absorption peaks exceed the measurement range. To confirm the frequency of these materials, hand-made apparatuses for the range of 27–40 GHz and 105–142 GHz were prepared (see the Experimental Section). The frequency of the absorption peak for $x = 0.67$ is observed at 35 GHz (Figure 2c, left). In contrast, the peak frequencies for $x = 0.22$ and 0.15 are observed at 115 and 126 GHz, respectively, and that for $x = 0.10$ is estimated to be observed at 147 GHz (Figure 2c, right). The absorption intensities of this series are strong (for example, the absorption intensity for $x = 0.40$ reaches 57 dB (99.9998%)).

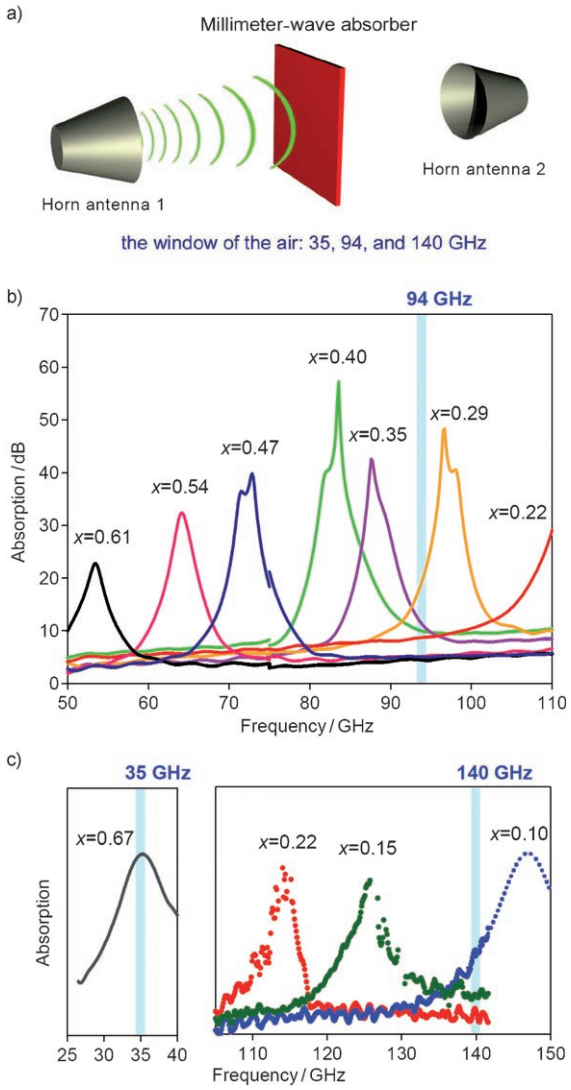

Figure 2. Millimeter-wave absorption properties of ε-$Ga_xFe_{2-x}O_3$. a) Schematic illustration of millimeter-wave absorption by the free-space technique. b) Millimeter-wave absorption for $x = 0.61$ (black), 0.54 (magenta), 0.47 (indigo), 0.40 (green), 0.35 (purple), 0.29 (orange), and 0.22 (red) in the range of 50–110 GHz measured at room temperature by the free-space technique. c) Left: Millimeter-wave absorption for $x = 0.67$ (gray) in the range 27–40 GHz. Right: Millimeter-wave absorption for $x = 0.22$ (red), 0.15 (dark green), and 0.10 (blue) using a hand-made apparatus in the range 105–142 GHz. The peak of the spectrum for $x = 0.10$ is supplemented by the line fitted by the Lorentzian function (dotted blue line). Blue belts show the windows of the air (35, 94, and 140 GHz).

Generally, in a ferromagnetic material with a magnetic anisotropy, the direction of magnetization is restricted around the magnetic easy axis, and the magnetization precesses around the easy axis. When an EM wave is applied to a ferromagnet, a ferromagnetic resonance (natural resonance) is observed.[9] The ferromagnetic resonance frequency (f_r) is proportional to the magnetocrystalline anisotropy field (H_a), which is expressed by $f_r = (\nu/2\pi)H_a$, where ν is the gyromagnetic ratio. When the sample consists of randomly oriented

magnetic particles with a uniaxial magnetic anisotropy, the H_a value is proportional to the H_c value. Figure 3 shows the relationship between the f_r and H_c values in the series presented here. As shown in the f_r and H_c plots, when the H_c value increases from 2.1 kOe ($x = 0.67$) to 15.9 kOe ($x = 0.10$), the f_r value also increases from 35 GHz to 147 GHz following the relationship $f_r = \alpha H_c$ ($\alpha = 9.63$, $R^2 = 0.945$). The upper limit of f_r of this series was estimated by using this relationship. The extrapolation of the relationship of f_r versus H_c suggests that the f_r value potentially reaches 193 ± 8 GHz in the sample for $H_c \rightarrow 20$ kOe (i.e. $x \rightarrow 0$).

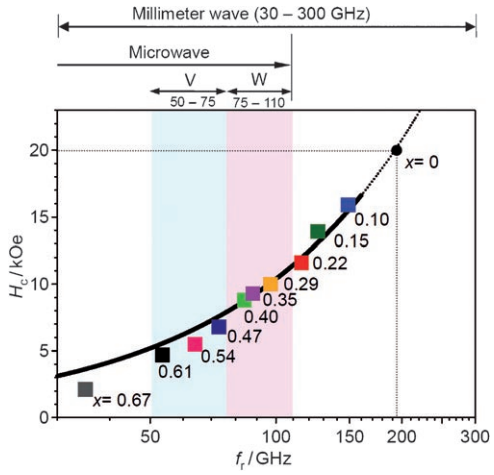

Figure 3. Relationship between f_r and H_c of ε-$Ga_xFe_{2-x}O_3$; the f_r and H_c values are related by $f_r = \alpha H_c$ ($\alpha = 9.63$, $R^2 = 0.945$). The extrapolation of this relation suggests that the f_r value should reach 193 ± 8 GHz at $H_c \rightarrow 20$ kOe (i.e. at $x \rightarrow 0$).

We have demonstrated a millimeter-wave absorber composed of ε-$Ga_xFe_{2-x}O_3$. This absorber can absorb millimeter waves in a wide range between 35 GHz and about 190 GHz. A millimeter-wave absorber of $f_r > 80$ GHz based on a magnetic material has not been reported to date. Furthermore, because our materials are a metal oxide, they are stable over long periods, and such millimeter-wave absorbers are advantageous for industrial applications. These new materials are suitable for an absorber to restrain the EMI (for example, a millimeter-wave absorber painted on the wall of an office, a private or medical room, or the body of a car, train, or airplane) and for an optoelectronic device to stabilize the EM transmittance (for example, a circulator and an isolator for millimeter waves of needless magnetic field).

Experimental Section

Materials: The samples for $x = 0.40$ were prepared by a combination method of the reverse-micelle and sol–gel techniques. Microemulsion systems were formed by cetyltrimethylammonium bromide (CTAB) and 1-butanol in *n*-octane with a H_2O/CTAB molar ratio of 31:1. The microemulsion containing an aqueous solution of $Fe(NO_3)_3$ (0.40 mol dm^{-3}) and $Ga(NO_3)_3$ (0.10 mol dm^{-3}) was mixed with another microemulsion containing 5 mol dm^{-3} NH_3 aqueous solution while rapidly stirring. Then tetraethoxysilane was added into the solution to yield a final molar ratio of [Si]/[Fe+Ga] = 1.5:1. This mixture was stirred for 20 h, and the materials were subsequently sintered at 1100 °C for 4 h in air. The SiO_2 matrices were etched by a NaOH solution for 24 h at 60 °C. The samples for $x = 0.10$, 0.15, 0.22, 0.29, 0.35, 0.47, 0.54, 0.61, and 0.67 were prepared by the sol–gel method. An aqueous solution of $Fe(NO_3)_3$ (0.48, 0.46, 0.44, 0.43, 0.41, 0.38, 0.37, 0.34, and 0.32 mol dm^{-3} for $x = 0.10$, 0.15, 0.22, 0.29, 0.35, 0.47, 0.54, 0.61, and 0.67, respectively) and $Ga(NO_3)_3$ (0.025, 0.038, 0.058, 0.073, 0.088, 0.12, 0.14, 0.16, and 0.18 mol dm^{-3} for $x = 0.10$, 0.15, 0.22, 0.29, 0.35, 0.47, 0.54, 0.61, and 0.67, respectively) was mixed with 5 mol dm^{-3} NH_3 aqueous solution while rapidly stirring. Then tetraethoxysilane was added into the solution to yield a final molar ratio of [Si]/[Fe+Ga] = 1.5:1. This mixture was stirred for 20 h. Afterwards, the materials were sintered at 1100 °C for 4 h in air. The SiO_2 matrices were etched by a NaOH solution for 24 h at 60 °C.

Characterization: Elemental analyses on the prepared samples were performed using inductively coupled plasma–atomic emission spectroscopy (ICP-AES, Jarrel-Ash, IRIS/AP). The TEM measurements were conducted using a JEOL 100CXII. The XRD measurements were conducted on a Rigaku RINT2100 with $Cu_{K\alpha}$ radiation ($\lambda = 1.5406$ Å) at 293 K within the range $19° \leq 2\theta \leq 100°$. Rietveld analyses were performed with the RIETAN-2000 program.[10] The magnetic properties were measured using a superconducting quantum interference device (SQUID) magnetometer (Quantum Design, MPMS 7).

EM absorption measurements: The EM absorption properties (V and W bands: 50–110 GHz) were measured at room temperature by using a free-space EM wave absorption measurement system (JFCC-HVS). Figure S6 in the Supporting Information shows a diagram of the measuring apparatus. The sample holder was a quartz cell of diameter 30 mm and height 10 mm. The fill ratios of the powder-form samples to the sample holder were as follows: 34 % ($x =$ 0.22), 35 (0.29), 41 (0.35), 40 (0.40), 42 (0.47), 40 (0.54), and 41 (0.61). The reflection coefficient (S_{11}) and permeability coefficient (S_{21}) were obtained. The absorption of the EM waves was calculated by the following equation: $A = -10\log[|S_{21}|^2/(1-|S_{11}|^2)]$ (dB). An absorption of 20 dB indicates that 99 % of the introduced EM waves are absorbed, which is the target value for EM absorbers from an industrial point of view. The preliminary measurement for $x = 0.67$ in the range of 27–40 GHz was carried out using a JFCC-HVS system. A hand-made apparatus to measure the samples for $x = 0.22$, 0.15, and 0.10 in the frequency range of 105–142 GHz was built by a network analyzer (562 scalar network analyzer, Anritsu), a signal generator, and a horn antenna. The sample holder had a diameter of 52 mm and a height of 5.5 mm. The fill ratio of the powder-form samples to the sample holder was 32 % ($x = 0.22$) and 25 % (0.10), respectively. The peak of the spectrum for $x = 0.10$ is supplemented by the line fitted by the Lorentzian function.

Received: July 6, 2007
Published online: October 17, 2007

Keywords: ferromagnetic resonance · magnetic properties · nanotechnology · sol–gel processes

[1] a) K. J. Vinoy, R. M. Jha, *Radar Absorbing Materials*, Kluwer, Boston, **1996**; b) A. Vilcot, B. Cabon, J. Chazelas, *Microwave Photonics*, Kluwer, Boston, **1996**; c) Y. Naito, K. Suetake, *IEEE Trans. Microwave Theory Tech.* **1971**, *19*, 65 – 72.

[2] a) C. H. Doan, S. Emami, A. M. Niknejad, R. W. Brodersen, *IEEE J. Solid-State Circuits* **2005**, *40*, 144 – 155; b) M. K. Chirala, C. Nguyen, *IEEE Trans. Microwave Theory Tech.* **2006**, *54*, 4218 – 4224; c) S. R. Bandi, C. Washburn, P. R. Mukund, J. Kolnik, K. Paradis, S. Howard, J. Burleson, *Solid-State Electron.* **2006**, *50*, 1450 – 1460; d) M. J. W. Rodwell, *High Speed Integrated Circuit Technology, towards 100 GHz Logic*, World Scientific,

Singapore, **2001**; e) K. Seemann, H. Leiste, V. A. Bekker, *J. Magn. Magn. Mater.* **2006**, *302*, 321 – 332.
[3] a) J. L. Snoek, *Physica* **1948**, *14*, 207 – 217; b) S. Yoshida, M. Sato, E. Sugawara, Y. Shimada, *J. Appl. Phys.* **1999**, *85*, 4636 – 4638; c) Z. G. Zhou, *Magnetic Ferrite Materials*, Science Press, Beijing, **1981**; d) K. Matsumoto, A. Kondo, T. Habu, K. Hayashi, O. Hashimoto, *Microwave Opt. Tech. Lett.* **2006**, *48*, 2065 – 2067.
[4] a) J. Jin, S. Ohkoshi, K. Hashimoto, *Adv. Mater.* **2004**, *16*, 48 – 51; b) S. Ohkoshi, S. Sakurai, J. Jin, K. Hashimoto, *J. Appl. Phys.* **2005**, *97*, 10K312/1 – 10K312/3; c) S. Sakurai, J. Jin, K. Hashimoto, S. Ohkoshi, *J. Phys. Soc. Jpn.* **2005**, *74*, 1946 – 1949.
[5] a) E. Tronc, C. Chanéac, J. P. Jolivet, *J. Solid State Chem.* **1998**, *139*, 93 – 104; b) E. Tronc, C. Chanéac, J. P. Jolivet, J. M. Grenèche, *J. Appl. Phys.* **2005**, *98*, 053901.
[6] a) M. Gich, C. Frontera, A. Roig, E. Taboada, E. Molins, H. R. Rechenberg, J. D. Ardisson, W. A. A. Macedo, C. Ritter, V. Hardy, J. Sort, V. Skumryev, J. Nogues, *Chem. Mater.* **2006**, *18*, 3889 – 3897; b) M. Popovici, M. Gich, D. Niznansky, A. Roig, C. Savii, L. Casas, E. Molins, K. Zaveta, C. Emache, J. Sort, S. Brion, G. Chouteau, J. Nogues, *Chem. Mater.* **2004**, *16*, 5542 – 5548.
[7] M. Kurmoo, J. Rehspringer, A. Hutlova, C. D'Orleans, S. Vilminot, C. Estournes, D. Niznansky, *Chem. Mater.* **2005**, *17*, 1106 – 1114.
[8] R. D. Shannon, *Acta Crystallogr. Sect. A* **1976**, *32*, 751 – 767.
[9] S. Chikazumi, *Physics of Ferromagnetism*, Oxford University Press, New York, **1997**.
[10] F. Izumi, T. Ikeda, *Mater. Sci. Forum* **2000**, *321–324*, 198 – 203.

